
Center Smoothing: Certified Robustness for Networks with Structured Outputs

Aounon Kumar
University of Maryland
aounon@umd.edu

Tom Goldstein
University of Maryland
tomg@cs.umd.edu

Abstract

The study of **provable adversarial robustness** has mostly been limited to classification tasks and models with **one-dimensional real-valued outputs**. We extend the scope of certifiable robustness to problems with **more general and structured outputs** like **sets, images, language**, etc. We model the output space as a metric space under a **distance/similarity function**, such as **intersection-over-union, perceptual similarity, total variation distance**, etc. Such models are used in many machine learning problems like **image segmentation, object detection, generative models, image/audio-to-text systems**, etc. Based on a robustness technique called **randomized smoothing**, our **center smoothing procedure** can produce models with the guarantee that the change in the output, as measured by the distance metric, remains small for any norm-bounded adversarial perturbation of the input. We apply our method to create certifiably robust models with disparate output spaces – from sets to images – and show that it yields meaningful certificates without significantly degrading the performance of the base model.

1 Introduction

The study of adversarial robustness in machine learning (ML) has gained a lot of attention ever since deep neural networks (DNNs) have been demonstrated to be vulnerable to adversarial attacks. These attacks are generated by making tiny perturbations of the input that can completely alter a model's predictions [56, 46, 23, 35]. They can significantly degrade the performance of a model, like an image classifier, and make it output almost any class of the attacker's choice. However, these attacks are not limited just to classification problems. They have also been shown to exist for DNNs with structured outputs like text, images, probability distributions, sets, etc. For instance, automatic speech recognition systems can be attacked with 100% success rate to output any phrase of the attackers choice [10]. Similar attacks can cause neural image captioning systems to produce specific target captions with high success-rate [11]. Quality of image segmentation models have been shown to degrade severely under adversarial attacks [2, 27, 30]. Facial recognition systems can be deceived to evade detection, impersonate authorized individuals and even render them completely ineffective [59, 55, 20]. Image reconstruction models have been targeted to introduce unwanted artefacts or miss important details, such as tumors in MRI scans, through adversarial inputs [1, 50, 8, 12]. Super-resolution systems can be made to generate distorted images that can in turn deteriorate the performance of subsequent tasks that rely on the high-resolution outputs [14, 63]. Deep neural network based policies in reinforcement learning problems also have been shown to succumb to imperceptible perturbations in the state observations [21, 29, 4, 48]. Such widespread presence of adversarial attacks is concerning as it threatens the use of deep neural networks in critical systems, such as facial recognition, self-driving vehicles, medical diagnosis, etc., where safety, security and reliability are of utmost importance.

Adversarial defenses have mostly focused on classification tasks [34, 6, 26, 17, 44, 25, 22]. Certified defenses based on convex-relaxation [61, 49, 53, 13, 54], interval-bound propagation [24, 28, 18, 47] and randomized smoothing [15, 36, 42, 51] that guarantee that the predicted class will remain the same in a certified region around the input point have also been studied. Compared to empirical robustness methods that are often shown to be broken by stronger attacks [9, 3, 58], procedures with provable robustness guarantees are of special importance to the study of robustness in ML as their guarantees hold regardless of improvements in attack strategies. Among these approaches, certified defenses based on randomized smoothing have been shown to scale up to high-dimensional inputs, such as images, and does not need to make assumptions about the underlying model. The robustness certificates produced by these defenses are probabilistic, meaning that they hold with high probability and not absolute certainty.

Unlike classification problems, where certificates guarantee that the predicted class remains unchanged under bounded-size perturbations, it is not immediately obvious what the goal of robustness should be for problems with structured outputs like images, text, sets, etc. While accuracy is the standard quality measure for classification, more complex tasks may require other quality metrics like total variation for images, intersection over union for object localization, earth-mover distance for distributions, etc. In general, neural networks can be cast as functions of the type $f : \mathbb{R}^k \rightarrow (M, d)$ which map a k dimensional real-valued space into a metric space M with distance function $d : M \times M \rightarrow \mathbb{R}_{\geq 0}$. In this work, we design a randomized smoothing based technique to obtain provable robustness for functions of this type with minimal assumptions on the distance metric d . We generate a robust version \bar{f} such that the change in its output, as measured by d , is small for a small change in its input. More formally, given an input x and an ℓ_2 -perturbation size ϵ_1 , we produce a value ϵ_2 with the guarantee that, with high probability,

$$\forall x' \text{ s.t. } \|x - x'\|_2 \leq \epsilon_1, d(\bar{f}(x), \bar{f}(x')) \leq \epsilon_2.$$

Our contributions: We develop *center smoothing*, a procedure to make functions like f provably robust against adversarial attacks. For a given input x , center smoothing samples a collection of points in the neighborhood of x using a Gaussian smoothing distribution, computes the function f on each of these points and returns the center of the smallest ball enclosing at least half the points in the output space (see figure 1). Computing the minimum enclosing ball in the output space is equivalent to solving the 1-center problem with outliers (hence the name of our procedure), which is an NP-complete problem for a general metric [52]. We approximate it by computing the point that has the smallest median distance to all the other points in the sample. We show that the output of the smoothed function is robust to input perturbations of bounded ℓ_2 -size. We restrict the input perturbations to be inside an ℓ_2 -ball as the main focus

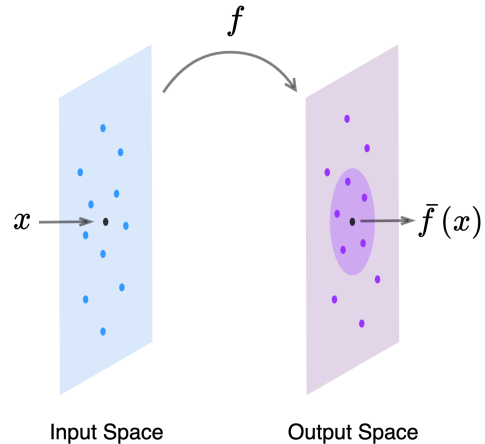


Figure 1: Center smoothing.

of this work is on the output space of f . However, our method does not critically rely on the ℓ_2 threat model or Gaussian smoothing noise, and can be adapted to other perturbations types and smoothing distributions. Although we define the output space as a metric, our proofs only require the symmetry property and triangle inequality to hold. Thus, center smoothing can also be applied to pseudometric distances that need not satisfy the identity of indiscernibles. Many distances defined for images, such as total variation, cosine distance, perceptual distances, etc., fall under this category. Center smoothing steps outside the world of ℓ_p metrics, and certifies robustness in metrics like IoU/Jaccard distance for object localization, and total-variation, which is a good measure of perceptual similarity for images. In our experiments, we show that this method can produce meaningful certificates for a wide variety of output metrics without significantly compromising the quality of the base model.

Related Work: Randomized smoothing has been extensively used for provable adversarial robustness in the classification setting to defend against different ℓ_p [15, 36, 51, 57, 43, 41, 37, 40] and non- ℓ_p [38, 39] threat models. Beyond classification, it has also been used for certifying the median output of regression models [62] and the expected softmax scores of neural networks [33]. Smoothing a bounded vector-valued function by taking the mean of the output vectors has been shown to have a

bounded Lipschitz constant when both input and output spaces are ℓ_2 -metrics [60]. Center smoothing does not require the base function to be bounded because the minimum enclosing ball is resistant to outliers. Moving an outlier point away from this ball does not affect the output of the smoothed function. On the other hand, smoothing techniques that compute the mean of the output samples are more susceptible to outliers as changing any of the samples can alter the mean. Recently, a provable defense for segmentation tasks was developed by certifying each individual pixel of the output using randomized smoothing [19]. Due to the accumulating uncertainty over individual certifications, it is difficult to produce guarantees for large images, often leading to certified outputs with ambiguous pixels. Center smoothing bypasses this challenge by directly certifying the similarity between a clean segmentation output and an adversarial one under a metric such as intersection over union.

2 Preliminaries and Notations

Given a function $f : \mathbb{R}^k \rightarrow (M, d)$ and a distribution \mathcal{D} over the input space \mathbb{R}^k , let $f(\mathcal{D})$ denote the probability distribution of the output of f in M when the input is drawn from \mathcal{D} . For a point $x \in \mathbb{R}^k$, let $x + \mathcal{P}$ denote the probability distribution of the points $x + \delta$ where δ is a smoothing noise drawn from a distribution \mathcal{P} over \mathbb{R}^k and let X be the random variable for $x + \mathcal{P}$. For elements in M , define $\mathcal{B}(z, r) = \{z' \mid d(z, z') \leq r\}$ as a ball of radius r centered at z . Define a smoothed version of f under \mathcal{P} as the center of the ball with the smallest radius in M that encloses at least half of the probability mass of $f(x + \mathcal{P})$, i.e.,

$$\bar{f}_{\mathcal{P}}(x) = \underset{z}{\operatorname{argmin}} r \text{ s.t. } \mathbb{P}[f(X) \in \mathcal{B}(z, r)] \geq \frac{1}{2}.$$

If there are multiple balls with the smallest radius satisfying the above condition, return one of the centers arbitrarily. Let $r_{\mathcal{P}}^*(x)$ be the value of the minimum radius. Hereafter, we ignore the subscripts and superscripts in the above definitions whenever they are obvious from context. In this work, we sample the noise vector δ from an i.i.d Gaussian distribution of variance σ^2 in each dimension, i.e., $\delta \sim \mathcal{N}(0, \sigma^2 I)$.

2.1 Gaussian Smoothing

Cohen et al. in 2019 showed that a classifier $h : \mathbb{R}^k \rightarrow \mathcal{Y}$ smoothed with a Gaussian noise $\mathcal{N}(0, \sigma^2 I)$ as,

$$\bar{h}(x) = \underset{c \in \mathcal{Y}}{\operatorname{argmax}} \mathbb{P}[h(x + \delta) = c],$$

where \mathcal{Y} is a set of classes, is certifiably robust to small perturbations in the input. Their certificate relied on the fact that, if the probability of sampling from the top class at x under the smoothing distribution is p , then for an ℓ_2 perturbation of size at most ϵ , the probability of the top class is guaranteed to be at least

$$p_{\epsilon} = \Phi(\Phi^{-1}(p) - \epsilon/\sigma), \quad (1)$$

where Φ is the CDF of the standard normal distribution $\mathcal{N}(0, 1)$. This bound applies to any $\{0, 1\}$ -function over the input space \mathbb{R}^k , i.e., if $\mathbb{P}[h(x) = 1] = p$, then for any ϵ -size perturbation x' , $\mathbb{P}[h(x') = 1] \geq p_{\epsilon}$.

We use this bound to generate robustness certificates for center smoothing. We identify a ball $\mathcal{B}(\bar{f}(x), R)$ of radius R enclosing a very high probability mass of the output distribution. One can define a function that outputs one if f maps a point to inside $\mathcal{B}(\bar{f}(x), R)$ and zero otherwise. The bound in (1) gives us a region in the input space such that for any point inside it, at least half of the mass of the output distribution is enclosed in $\mathcal{B}(\bar{f}(x), R)$. We show in section 3 that the output of the smoothed function for a perturbed input is guaranteed to be within a constant factor of R from the output of the original input.

3 Center Smoothing

As defined in section 2, the output of \bar{f} is the center of the smallest ball in the output space that encloses at least half the probability mass of the $f(x + \mathcal{P})$. Thus, in order to significantly change the output, an adversary has to find a perturbation such that a majority of the neighboring points map far away from $\bar{f}(x)$. However, for a function that is roughly accurate on most points around x , a

small perturbation in the input cannot change the output of the smoothed function by much, thereby making it robust.

For an ℓ_2 perturbation size of ϵ_1 of an input point x , let R be the radius of a ball around $\bar{f}(x)$ that encloses more than half the probability mass of $f(x' + \mathcal{P})$ for all x' satisfying $\|x - x'\|_2 \leq \epsilon_1$, i.e.,

$$\forall x' \text{ s.t. } \|x - x'\|_2 \leq \epsilon_1, \mathbb{P}[f(X') \in \mathcal{B}(\bar{f}(x), R)] > \frac{1}{2}, \quad (2)$$

where $X' \sim x' + \mathcal{P}$. Basically, R is the radius of a ball around $\bar{f}(x)$ that contains at least half the probability mass of $f(x' + \mathcal{P})$ for any ϵ_1 -size perturbation x' of x . Then, we have the following robustness guarantee on \bar{f} :

Theorem 1. For all x' such that $\|x - x'\|_2 \leq \epsilon_1$,

$$d(\bar{f}(x), \bar{f}(x')) \leq 2R.$$

Proof. Consider the balls $\mathcal{B}(\bar{f}(x'), r^*(x'))$ and $\mathcal{B}(\bar{f}(x), R)$ (see figure 2). From the definition of $r^*(x')$ and R , we know that the sum of the probability masses of $f(x' + \mathcal{P})$ enclosed by the two balls must be strictly greater than one. Thus, they must have an element y in common. Since d satisfies the triangle inequality, we have:

$$\begin{aligned} d(\bar{f}(x), \bar{f}(x')) &\leq d(\bar{f}(x), y) + d(y, \bar{f}(x')) \\ &\leq R + r^*(x'). \end{aligned}$$

Since, the ball $\mathcal{B}(\bar{f}(x), R)$ encloses more than half of the probability mass of $f(x + \mathcal{P})$, the minimum ball with at least half the probability mass cannot have a radius greater than R , i.e., $r^*(x') \leq R$. Therefore, $d(\bar{f}(x), \bar{f}(x')) \leq 2R$. \square

The above result, in theory, gives us a smoothed version of f with a provable guarantee of robustness. However, in practice, it may not be feasible to obtain \bar{f} just from samples of $f(x + \mathcal{P})$. Instead, we will use some procedure that approximates the smoothed output with high probability. For some $\Delta \in [0, 1/2]$, let $\hat{r}(x, \Delta)$ be the radius of the smallest ball that encloses at least $1/2 + \Delta$ probability mass of $f(x + \mathcal{P})$, i.e.,

$$\hat{r}(x, \Delta) = \min_{z'} r \text{ s.t. } \mathbb{P}[f(X) \in \mathcal{B}(z', r)] \geq \frac{1}{2} + \Delta.$$

Now define a probabilistic approximation $\hat{f}(x)$ of the smoothed function \bar{f} to be a point $z \in M$, which with probability at least $1 - \alpha_1$ (for $\alpha_1 \in [0, 1]$), encloses at least $1/2 - \Delta$ probability mass of $f(x + \mathcal{P})$ within a ball of radius $\hat{r}(x, \Delta)$. Formally, $\hat{f}(x)$ is a point $z \in M$, such that, with at least $1 - \alpha_1$ probability,

$$\mathbb{P}[f(X) \in \mathcal{B}(z, \hat{r}(x, \Delta))] \geq \frac{1}{2} - \Delta.$$

Defining \hat{R} to be the radius of a ball centered at $\hat{f}(x)$ that satisfies:

$$\forall x' \text{ s.t. } \|x - x'\|_2 \leq \epsilon_1, \mathbb{P}[f(X') \in \mathcal{B}(\hat{f}(x), \hat{R})] > \frac{1}{2} + \Delta, \quad (3)$$

we can write a probabilistic version of theorem 1,

Theorem 2. With probability at least $1 - \alpha_1$,

$$\forall x' \text{ s.t. } \|x - x'\|_2 \leq \epsilon_1, d(\hat{f}(x), \hat{f}(x')) \leq 2\hat{R},$$

The proof of this theorem is in the appendix, and logically parallels the proof of theorem 1.

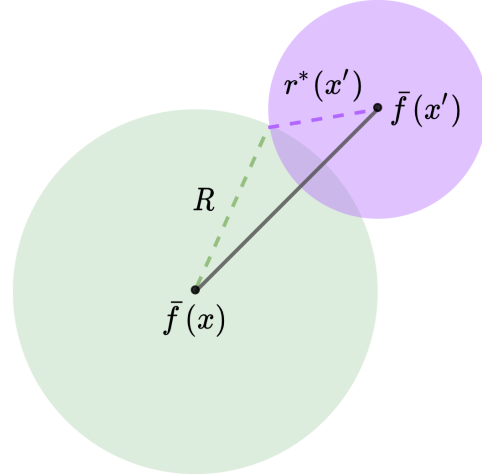


Figure 2: Robustness guarantee.

Algorithm 1 Smooth

Input: $x \in \mathbb{R}^k, \sigma, \Delta, \alpha_1$.
Output: $z \in M$.
Set $Z = \{z_i\}_{i=1}^n$ s.t. $z_i \sim f(x + \mathcal{N}(0, \sigma^2 I))$.
Set $\Delta_1 = \sqrt{\ln(2/\alpha_1)/2n}$.
Compute $z = \beta\text{-MEB}(Z, 1/2)$.
Re-sample Z .
Compute p_{Δ_1} .
Set $\Delta_2 = 1/2 - p_{\Delta_1}$.
If $\Delta < \max(\Delta_1, \Delta_2)$, discard z and abstain.

Algorithm 2 Certify

Input: $x \in \mathbb{R}^k, \epsilon_1, \sigma, \Delta, \alpha_1, \alpha_2$.
Output: $\epsilon_2 \in \mathbb{R}$.
Compute $\hat{f}(x)$ using algorithm 1.
Set $Z = \{z_i\}_{i=1}^m$ s.t. $z_i \sim f(x + \mathcal{N}(0, \sigma^2 I))$.
Compute $\tilde{\mathcal{R}} = \{d(\hat{f}(x), f(z_i)) \mid z_i \in Z\}$.
Set $p = \Phi(\Phi^{-1}(1/2 + \Delta) + \epsilon_1/\sigma)$.
Set $q = p + \sqrt{\ln(1/\alpha_2)/2m}$.
Set $\hat{R} = q\text{th-quantile of } \tilde{\mathcal{R}}$.
Set $\epsilon_2 = (1 + \beta)\hat{R}$.

3.1 Computing \hat{f}

For an input x and a given value of Δ , sample n points independently from a Gaussian distribution $x + \mathcal{N}(0, \sigma^2 I)$ around the point x and compute the function f on each of these points. Let $Z = \{z_1, z_2, \dots, z_n\}$ be the set of n samples of $f(x + \mathcal{N}(0, \sigma^2 I))$ produced in the output space. Compute the minimum enclosing ball $\mathcal{B}(z, r)$ that contains at least half of the points in Z . The following lemma bounds the radius r of this ball by the radius of the smallest ball enclosing at least $1/2 + \Delta_1$ probability mass of the output distribution (proof in appendix).

Lemma 1. *With probability at least $1 - e^{-2n\Delta_1^2}$,*

$$r \leq \hat{r}(x, \Delta_1).$$

Now, sample a fresh batch of n random points. Let $p_{\Delta_1} = \rho - \Delta_1$, where ρ is the fraction of points that fall inside $\mathcal{B}(z, r)$. Then, by Hoeffding's inequality, with probability at least $1 - e^{-2n\Delta_1^2}$,

$$\mathbb{P}[f(X) \in \mathcal{B}(z, r)] \geq p_{\Delta_1}.$$

Let $\Delta_2 = 1/2 - p_{\Delta_1}$. If $\max(\Delta_1, \Delta_2) \leq \Delta$, the point z satisfies the conditions in the definition of \hat{f} , with at least $1 - 2e^{-2n\Delta_1^2}$ probability. If $\max(\Delta_1, \Delta_2) > \Delta$, discard the computed center z and abstain. In our experiments, we select Δ_1, n and α_1 appropriately so that the above process succeeds easily.

Computing the minimum enclosing ball $\mathcal{B}(z, r)$ exactly can be computationally challenging, as for certain metrics, it is known to be NP-complete [52]. Instead, we approximate it by computing a ball $\beta\text{-MEB}(Z, 1/2)$ that contains at least half the points in Z , but has a radius that is within a β factor of the optimal radius r . We modify theorem 1 to account for this approximation (see appendix for proof).

Theorem 3. *With probability at least $1 - \alpha_1$,*

$$\forall x' \text{ s.t. } \|x - x'\|_2 \leq \epsilon_1, \quad d(\hat{f}(x), \hat{f}(x')) \leq (1 + \beta)\hat{R}$$

where $\alpha_1 = 2e^{-2n\Delta_1^2}$.

We use a simple approximation that works for all metrics and achieves an approximation factor of two, producing a certified radius of $3\hat{R}$. It computes a point from the set Z , instead of a general point in M , that has the minimum median distance from all the points in the set (including itself). This can be achieved using $O(n^2)$ pair-wise distance computations. To see how the factor 2-approximation is achieved, consider the optimal ball with radius r . By triangle inequality of d , each pair of points is at most $2r$ distance from each other. Thus, a ball with radius $2r$, centered at any one of these points will cover every other point in the optimal ball. Better approximations can be obtained for specific norms, e.g., there exists a $(1 + \epsilon)$ -approximation algorithm for the ℓ_2 norm [7]. For graph distances or when the support of the output distribution is a small discrete set of points, the optimal radius can be computed exactly using the above algorithm. The smoothing procedure is outlined in algorithm 1.

3.2 Certifying \hat{f}

Given an input x , compute $\hat{f}(x)$ as described above. Now, we need to compute a radius \hat{R} that satisfies condition 3. As per bound 1, in order to maintain a probability mass of at least $1/2 + \Delta$ for

any ϵ_1 -size perturbation of x , the ball $\mathcal{B}(\hat{f}(x), \hat{R})$ must enclose at least

$$p = \Phi \left(\Phi^{-1} \left(\frac{1}{2} + \Delta \right) + \frac{\epsilon_1}{\sigma} \right) \quad (4)$$

probability mass of $f(x + \mathcal{P})$. Again, just as in the case of estimating \bar{f} , we may only compute \hat{R} from a finite number of samples m of the distribution $f(x + \mathcal{P})$. For each sample $z_i \sim x + \mathcal{P}$, we compute the distance $d(\hat{f}(x), f(z_i))$ and set \hat{R} to be the q th-quantile \tilde{R}_q of these distances for a q that is slightly greater than p (see equation 5 below). The q th-quantile \tilde{R}_q is a value larger than at least q fraction of the samples. We set q as,

$$q = p + \sqrt{\frac{\ln(1/\alpha_2)}{2m}}, \quad (5)$$

for some small $\alpha_2 \in [0, 1]$. This guarantees that, with high probability, the ball $\mathcal{B}(\hat{f}(x), \tilde{R}_q)$ encloses at least p fraction of the probability mass of $f(x + \mathcal{P})$. We prove the following lemma by bounding the cumulative distribution function of the distances of $f(z_i)$ s from $\hat{f}(x)$ using the Dvoretzky–Kiefer–Wolfowitz inequality.

Lemma 2. *With probability $1 - \alpha_2$,*

$$\mathbb{P} \left[f(X) \in \mathcal{B}(\hat{f}(x), \tilde{R}_q) \right] > p.$$

Combining with theorem 3, we have the final certificate:

$$\forall x' \text{ s.t. } \|x - x'\|_2 \leq \epsilon_1, \quad d(\hat{f}(x), \hat{f}(x')) \leq (1 + \beta)\hat{R},$$

with probability at least $1 - \alpha$, for $\alpha = \alpha_1 + \alpha_2$. In our experiments, we set $\alpha_1 = \alpha_2 = 0.005$ to achieve an overall success probability of $1 - \alpha = 0.99$, and calculate the required Δ_1, Δ_2 and q values accordingly. We set Δ to be as small as possible without violating $\max(\Delta_1, \Delta_2) \leq \Delta$ too often. We use a $\beta = 2$ -approximation for computing the minimum enclosing ball in the smoothing step. Algorithm 2 provides the pseudocode for the certification procedure.

4 Relaxing Metric Requirements

Although we defined our procedure for metric outputs, our analysis does not critically use all the properties of a metric. For instance, we do not require $d(z_1, z_2)$ to be strictly greater than zero for $z_1 \neq z_2$. An example of such a distance measure is the total variation distance that returns zero for two vectors that differ by a constant amount on each coordinate. Our proofs do implicitly use the symmetry property, but asymmetric distances can be converted to symmetric ones by taking the sum or the max of the distances in either directions. Perhaps the most important property of metrics that we use is the triangle inequality as it is critical for the robustness guarantee of the smoothed function. However, even this constraint may be partially relaxed. It is sufficient for the distance function d to satisfy the triangle inequality approximately, i.e., $d(a, c) \leq \gamma(d(a, b) + d(b, c))$, for some constant γ . The theorems and lemmas can be adjusted to account for this approximation, e.g., the bound in theorem 1 will become $2\gamma R$. A commonly used distance measure for comparing images and documents is the cosine distance defined as the inner-product of two vectors after normalization. This distance can be show to be proportional to the squared Euclidean distance between the normalized vectors which satisfies the relaxed version of triangle inequality for $\gamma = 2$.

These relaxations extend the scope of center smoothing to many commonly used distance measures that need not necessarily satisfy all the metric properties. For instance, perceptual distance metrics measure the distance between two images in some feature space rather than image space. Such distances align well with human judgements when the features are extracted from a deep neural network [65] and are considered more natural measures for image similarity. For two images I_1 and I_2 , let $\phi(I_1)$ and $\phi(I_2)$ be their feature representations. Then, for a distance function d in the feature space that satisfies the relaxed triangle inequality, we can define a distance function $d_\phi(I_1, I_2) = d(\phi(I_1), \phi(I_2))$ in the image space, which also satisfies the relaxed triangle inequality. For any image I_3 ,

$$\begin{aligned} d_\phi(I_1, I_2) &= d(\phi(I_1), \phi(I_2)) \\ &\leq \gamma (d(\phi(I_1), \phi(I_3)) + d(\phi(I_3), \phi(I_2))) \\ &= \gamma (d_\phi(I_1, I_3) + d_\phi(I_3, I_2)). \end{aligned}$$

5 Experiments

We apply center smoothing to certify a wide range of output metrics: Jaccard distance based on intersection over union (IoU) of sets, total variation distances for images, and perceptual distance. We certify the bounding box generated by a face detector – a key component of most facial recognition systems – by guaranteeing the minimum overlap (measured using IoU) it must have with the output under an adversarial perturbation of the input. For instance, if $\epsilon_1 = 0.2$, the Jaccard distance (1-IoU) is guaranteed to be bounded by 0.2, which implies that the bounding box of a perturbed image must have at least 80% overlap with that of the clean image. We use a pre-trained face detection model for this experiment. We certify the perceptual distance of the output of a generative model (trained on ImageNet) that produces 128×128 RGB images using a high-dimensional version of the smoothing procedure Smooth-HD described in the appendix. For total variation distance, we use simple, easy-to-train convolutional neural network based dimensionality reduction (autoencoder) and image reconstruction models. Our goal is to demonstrate the effectiveness of our method for a wide range of applications and so, we place less emphasis on the performance of the underlying models being smoothed. In each case, we show that our method is capable of generating certified guarantees without significantly degrading the performance of the underlying model. We provide additional experiments for other metrics and parameter settings in the appendix.

As is common in the randomized smoothing literature, we train our base models (except for the pre-trained ones) on noisy data with different noise levels $\sigma_{train} = 0.1, 0.2, \dots, 0.5$ to make them more robust to input perturbations. We keep the smoothing noise σ of the robust model same as the training noise σ_{train} of the base model. We use $n = 10^4$ samples to estimate the smoothed function and $m = 10^6$ samples to generate certificates, unless stated otherwise. We set $\Delta = 0.05$, $\alpha_1 = 0.005$ and $\alpha_2 = 0.005$ as discussed in previous sections. We grow the smoothing noise σ linearly with the input perturbation ϵ_1 . Specifically, we maintain $\epsilon_1 = h\sigma$ for different values of $h = 2, 1$ and 1.5 in our experiments. We plot the median certified output radius ϵ_2 and the median smoothing error, defined as the distance between the outputs of the base model and the smoothed model $d(f(x), \hat{f}(x))$, of fifty random test examples for different values of ϵ_1 . In all our experiments, we observe that both these quantities increase as the input radius ϵ_1 increases, but the smoothing error remains significantly below the certified output radius. Also, increasing the value of h improves the quality of the certificates (lower ϵ_2). This could be due to the fact that for a higher h , the smoothing noise σ is lower (keeping ϵ_1 constant), which means that the radius of the minimum enclosing ball in the output space is smaller leading to a tighter certificate. However, setting h too high can cause the value of q in equation 5 to exceed one (q depends on p , which in turn depends on h in eq. 4), leading the certification procedure (algorithm 2) to fail. We ran all our experiments on a single NVIDIA GeForce RTX 2080 Ti GPU in an internal cluster. Each of the fifty examples we certify took somewhere between 1-3 minutes depending on the underlying model.

5.1 Jaccard distance

It is known that facial recognition systems can be deceived to evade detection, impersonate authorized individuals and even render completely ineffective [59, 55, 20]. Most facial recognition systems first detect a region that contains a persons face, e.g. a bounding box, and then uses facial features to identify the individual in the image. To evade detection, an attacker may seek to degrade the quality of the bounding boxes produced by the detector and can even cause it to detect no box at all. Bounding boxes are often interpreted as sets and their quality is measured as the amount of overlap with the desired output. When no box is output, we say the overlap is zero. The overlap between two sets is defined as the ratio of the size of the intersection between them to the size of their union (IoU). Thus, to certify the robustness of the output of a face detector, it makes sense to bound the worst-case IoU of the output of an adversarial input to that of a clean input. The corresponding distance function, known as Jaccard distance, is defined as $1 - IoU$ which defines a metric over the universe of sets.

$$IoU(A, B) = \frac{|A \cap B|}{|A \cup B|}, \quad d_J(A, B) = 1 - IoU(A, B) = 1 - \frac{|A \cap B|}{|A \cup B|}.$$

In this experiment, we certify the output of a pre-trained face detection model MTCNN [64] on the CelebA face dataset [45]. We set $n = 5000$ and $m = 10000$, and use default values for other parameters discussed above. Figure 3a plots the certified output radius ϵ_2 and the smoothing error for $h = \epsilon_1/\sigma = 1$ and 2 for $\epsilon_1 = 0.1, 0.2, \dots, 0.5$. Certifying the Jaccard distance allows us to certify

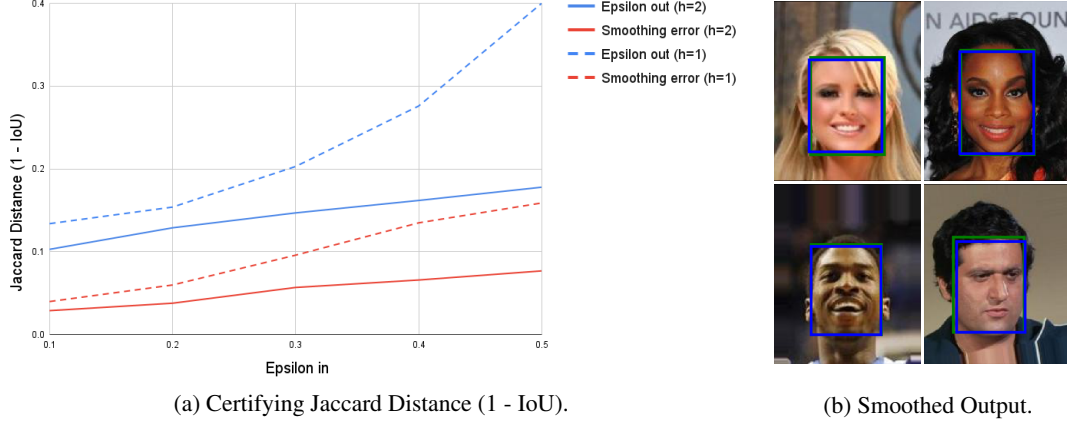


Figure 3: Face Detection on CelebA using MTCNN detector: Part (a) plots the certified output radius ϵ_2 and the smoothing error for $h = 1$ and 2 . Part (b) compares the smoothed output (blue box) to the output of the base model (green box, mostly hidden behind the blue box) showing a significant overlap.

IoU as well, e.g., for $h = 2$, ϵ_2 is consistently below 0.2 which means that even the worst bounding box under adversarial perturbation of the input has an overlap of at least 80% with the box for the clean input. The low smoothing error shows that the performance of the base model does not drop significantly as the actual output of the smoothed model has a large overlap with that of the base model. Figure 3b compares the outputs of the smoothed model (blue box) and the base model (green box). For most of the images, the blue box overlaps with the green one almost perfectly.

5.2 Perceptual Distance

Deep generative models like GANs and VAEs have been shown to be vulnerable to adversarial attacks [31]. One attack model is to produce an adversarial example that is close to the original input in the latent space, measured using ℓ_2 -norm. The goal is to make the model generate a different looking image using a latent representation that is close to that of the original image. We apply center smoothing to a generative adversarial network BigGAN pre-trained on ImageNet images [5]. We use the version of the GAN that generates 128×128 resolution ImageNet images from a set of 128 latent variables. Since we are interested in producing similar looking images for similar latent representations, a good output metric would be the perceptual distance between two images measured by LPIPS metric [65]. This distance function takes in two images, passes them through a deep neural network, such as VGG, and computes a weighted sum of the square of the differences of the activations (after some normalization) produced by the two images. The process can be thought of as generating two feature vectors ϕ_1 and ϕ_2 for the two input images I_1 and I_2 respectively, then computing a weighted sum of the element-wise square of the differences between the two feature vectors, i.e.,

$$d(I_1, I_2) = \sum_i w_i (\phi_{1i} - \phi_{2i})^2$$

The square of differences metric can be shown to follow the relaxed triangle inequality for $\gamma = 2$. Therefore, the final bound on the certified output radius will be $\gamma(1 + 2\gamma)\hat{R} = 10\hat{R}$. Figure 4a plots the median smoothing error and certified output radius ϵ_2 for fifty randomly picked latent vectors for $\epsilon_1 = 0.01, 0.02, \dots, 0.05$ and $h = 1, 1.5$. For these experiments, we set $n = 2000$, $m = 10^4$ and $\Delta = 0.8$. We use the modified smoothing procedure Smooth-HD (see appendix) for high-dimensional outputs with a small batch size of 150 to accommodate the samples in memory. It takes about three minutes to smooth and certify each input on a single NVIDIA GeForce RTX 2080 Ti GPU in an internal cluster. Due to the higher factor of ten in the certified output radius in this case compared to our other experiments where the factor is three, the certified output radius increases faster with the input radius ϵ_1 , but the smoothing error remains low showing that, in practice, the method does not significantly degrade the performance of the base model. Figure 4b shows that, visually, the smoothed output is not very different from the output of the base model. The input radii we certify for are lower in this case than our other experiments due to the low dimensionality (only 128 dimensions) of the input (latent) space as compared to the input (image) spaces in our other experiments.

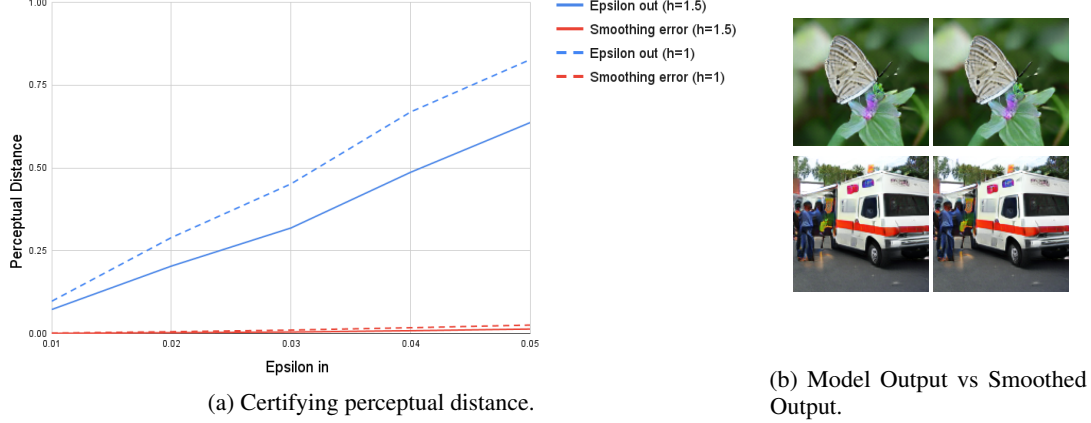


Figure 4: Generative model for ImageNet: Part (a) plots the certified output radius ϵ_2 and the smoothing error for $h = 1$ and 1.5 . Part (b) compares the output of the base model to that of the smoothed model.

5.3 Total Variation Distance

The total variation norm of a vector x is defined as the sum of the magnitude of the difference between pairs of coordinates defined by a *neighborhood* set N . For a 1-dimensional array x with k elements, one can define the neighborhood as the set of consecutive elements.

$$TV(x) = \sum_{(i,j) \in N} |x_i - x_j|, \quad TV_{1D}(x) = \sum_{i=1}^{k-1} |x_i - x_{i+1}|.$$

Similarly, for a grayscale image represented by a $h \times w$ 2-dimensional array x , the neighborhood can be defined as the next element (pixel) in the row/column. In case of an RGB image, the difference between the neighboring pixels is a vector, whose magnitude can be computed using an ℓ_p -norm. For, our experiments we use the ℓ_1 -norm.

$$TV_{RGB}(x) = \sum_{i=1}^{h-1} \sum_{j=1}^{w-1} \|x_{i,j} - x_{i+1,j}\|_1 + \|x_{i,j} - x_{i,j+1}\|_1$$

The total variation distance between two images I_1 and I_2 can be defined as the total variation norm of the difference $I_1 - I_2$, i.e., $TVD(I_1, I_2) = TV(I_1 - I_2)$. The above distance defines a pseudometric over the space of images as it satisfies the symmetry property and the triangle inequality, but may violate the identity of indiscernibles as an image obtained by adding the same value to all the pixel intensities has a distance of zero from the original image. However, as noted in section 4, our certificates hold even for this setting.

We certify total variation distance for the problems of dimensionality reduction and image reconstruction on MNIST [16] and CIFAR-10 [32]. The base-model for dimensionality reduction is an autoencoder that uses convolutional layers in its encoder module to map an image down to a small number of latent variables. The decoder applies a set of de-convolutional operations to reconstruct the same image. We insert batch-norm layers in between these operations to improve performance. For image reconstruction, the goal is to recover an image from small number of measurements of the original image. We apply a transformation defined by Gaussian matrix A on each image to obtain the measurements. The base model tries to reconstruct the original image from the measurements. The attacker, in this case, is assumed to add a perturbation in the measurement space instead of the image space (as in dimensionality reduction). The model first reverts the measurement vector to a vector in the image space by simply applying the pseudo-inverse of A and then passes it through a similar autoencoder model as for dimensionality reduction. We present results for $\epsilon_1 = 0.2, 0.4, \dots, 1.0$ and $h = 2, 1.5$ and use 256 latent dimensions and measurements for these experiments in figure 5. To put these plots in perspective, the maximum TVD between two CIFAR-10 images could be $6 \times 31 \times 31 = 5766$ and between MNIST images could be $2 \times 27 \times 27 = 1458$ (pixel values between 0 and 1).

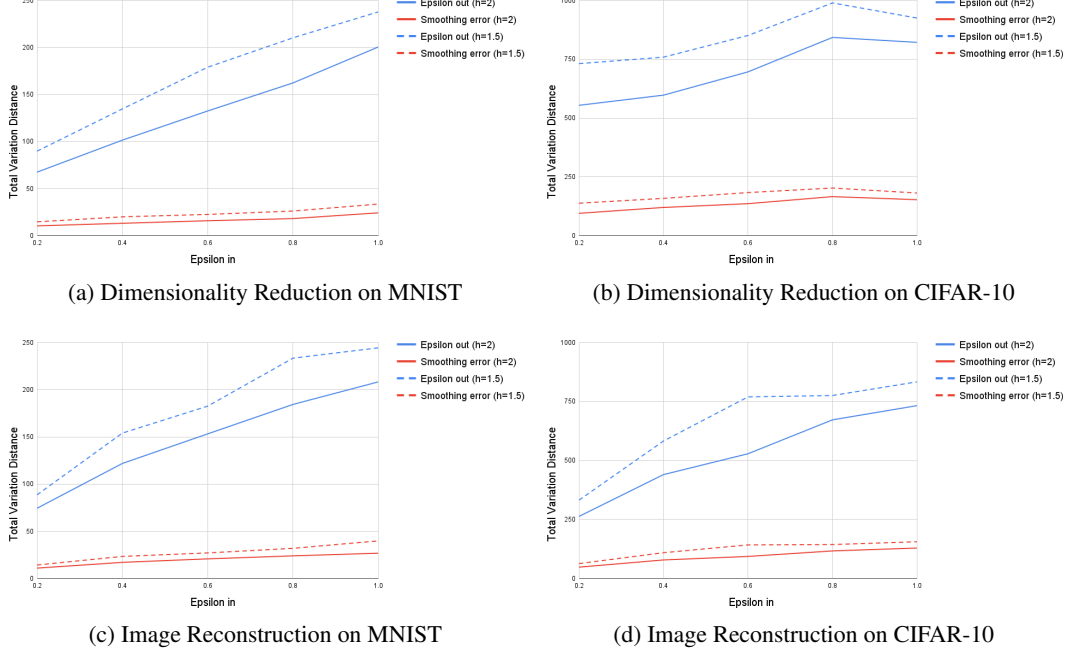


Figure 5: Certifying Total Variation Distance

6 Conclusion

Provable adversarial robustness can be extended beyond classification tasks to problems with structured outputs. We design a smoothing-based procedure that can make a model of this kind provably robust against norm bounded adversarial perturbations of the input. In our experiments, we demonstrate that this method can generate meaningful certificates under a wide variety of distance metrics in the output space without significantly compromising the quality of the base model. We also note that the metric requirements on the distance measure can be partially relaxed in exchange for weaker certificates.

We focus on ℓ_2 -norm bounded adversaries and the Gaussian smoothing distribution. An important direction for future investigation could be whether this method can be generalised beyond ℓ_p -adversaries to more natural threat models, e.g., adversaries bounded by total variation distance, perceptual distance, cosine distance, etc. Center smoothing does not critically rely on the shape of the smoothing distribution or the threat model. Thus, improvements in these directions could potentially be coupled with our method to further broaden the scope of provable robustness in machine learning.

7 Acknowledgements

This work was supported by the AFOSR MURI program, DARPA GARD, the Office of Naval Research, and the National Science Foundation Division of Mathematical Sciences.

References

- [1] Vegard Antun, Francesco Renna, Clarice Poon, Ben Adcock, and Anders C. Hansen. On instabilities of deep learning in image reconstruction - does AI come at a cost? *CoRR*, abs/1902.05300, 2019. URL <http://arxiv.org/abs/1902.05300>.
- [2] Anurag Arnab, Ondrej Miksik, and Philip H. S. Torr. On the robustness of semantic segmentation models to adversarial attacks. *CoRR*, abs/1711.09856, 2017. URL <http://arxiv.org/abs/1711.09856>.
- [3] Anish Athalye, Nicholas Carlini, and David Wagner. Obfuscated gradients give a false sense of security: Circumventing defenses to adversarial examples. In Jennifer Dy and Andreas Krause, editors, *Proceedings of the 35th International Conference on Machine Learning*, volume 80 of *Proceedings of Machine Learning Research*, pages 274–283, Stockholmsmässan, Stockholm Sweden, 10–15 Jul 2018. PMLR.
- [4] Vahid Behzadan and Arslan Munir. Vulnerability of deep reinforcement learning to policy induction attacks. In Petra Perner, editor, *Machine Learning and Data Mining in Pattern Recognition - 13th International Conference, MLDM 2017, New York, NY, USA, July 15-20, 2017, Proceedings*, volume 10358 of *Lecture Notes in Computer Science*, pages 262–275. Springer, 2017. doi: 10.1007/978-3-319-62416-7_19. URL https://doi.org/10.1007/978-3-319-62416-7_19.
- [5] Andrew Brock, Jeff Donahue, and Karen Simonyan. Large scale GAN training for high fidelity natural image synthesis. In *7th International Conference on Learning Representations, ICLR 2019, New Orleans, LA, USA, May 6-9, 2019*. OpenReview.net, 2019. URL <https://openreview.net/forum?id=B1xsqj09Fm>.
- [6] Jacob Buckman, Aurko Roy, Colin Raffel, and Ian J. Goodfellow. Thermometer encoding: One hot way to resist adversarial examples. In *6th International Conference on Learning Representations, ICLR 2018, Vancouver, BC, Canada, April 30 - May 3, 2018, Conference Track Proceedings*, 2018.
- [7] Mihai Bundeineddoiu, Sariel Har-Peled, and Piotr Indyk. Approximate clustering via core-sets. In *Proceedings of the Thirty-Fourth Annual ACM Symposium on Theory of Computing, STOC '02*, page 250–257, New York, NY, USA, 2002. Association for Computing Machinery. ISBN 1581134959. doi: 10.1145/509907.509947. URL <https://doi.org/10.1145/509907.509947>.
- [8] Francesco Calivá, Kaiyang Cheng, Rutwik Shah, and Valentina Pedoia. Adversarial robust training in mri reconstruction. *arXiv preprint arXiv:2011.00070*, 2020.
- [9] Nicholas Carlini and David A. Wagner. Adversarial examples are not easily detected: Bypassing ten detection methods. In *Proceedings of the 10th ACM Workshop on Artificial Intelligence and Security, AISec@CCS 2017, Dallas, TX, USA, November 3, 2017*, pages 3–14, 2017.
- [10] Nicholas Carlini and David A. Wagner. Audio adversarial examples: Targeted attacks on speech-to-text. *CoRR*, abs/1801.01944, 2018. URL <http://arxiv.org/abs/1801.01944>.
- [11] Hongge Chen, Huan Zhang, Pin-Yu Chen, Jinfeng Yi, and Cho-Jui Hsieh. Show-and-fool: Crafting adversarial examples for neural image captioning. *CoRR*, abs/1712.02051, 2017. URL <http://arxiv.org/abs/1712.02051>.
- [12] Kaiyang Cheng, Francesco Calivá, Rutwik Shah, Misung Han, Sharmila Majumdar, and Valentina Pedoia. Addressing the false negative problem of deep learning mri reconstruction models by adversarial attacks and robust training. In Tal Arbel, Ismail Ben Ayed, Marleen de Bruijne, Maxime Descoteaux, Herve Lombaert, and Christopher Pal, editors, *Proceedings of the Third Conference on Medical Imaging with Deep Learning*, volume 121 of *Proceedings of Machine Learning Research*, pages 121–135, Montreal, QC, Canada, 06–08 Jul 2020. PMLR. URL <http://proceedings.mlr.press/v121/cheng20a.html>.
- [13] Ping-yeh Chiang, Renkun Ni, Ahmed Abdelkader, Chen Zhu, Christoph Studer, and Tom Goldstein. Certified defenses for adversarial patches. In *8th International Conference on Learning Representations*, 2020.
- [14] Jun-Ho Choi, Huan Zhang, Jun-Hyuk Kim, Cho-Jui Hsieh, and Jong-Seok Lee. Evaluating robustness of deep image super-resolution against adversarial attacks. In *2019 IEEE/CVF International Conference on Computer Vision, ICCV 2019, Seoul, Korea (South), October*

- 27 - November 2, 2019, pages 303–311. IEEE, 2019. doi: 10.1109/ICCV.2019.00039. URL <https://doi.org/10.1109/ICCV.2019.00039>.
- [15] Jeremy Cohen, Elan Rosenfeld, and Zico Kolter. Certified adversarial robustness via randomized smoothing. In Kamalika Chaudhuri and Ruslan Salakhutdinov, editors, *Proceedings of the 36th International Conference on Machine Learning*, volume 97 of *Proceedings of Machine Learning Research*, pages 1310–1320, Long Beach, California, USA, 09–15 Jun 2019. PMLR.
 - [16] Li Deng. The mnist database of handwritten digit images for machine learning research [best of the web]. *IEEE Signal Processing Magazine*, 29(6):141–142, 2012. doi: 10.1109/MSP.2012.2211477.
 - [17] Guneet S. Dhillon, Kamyar Azizzadenesheli, Zachary C. Lipton, Jeremy Bernstein, Jean Kossaifi, Aran Khanna, and Animashree Anandkumar. Stochastic activation pruning for robust adversarial defense. In *6th International Conference on Learning Representations, ICLR 2018, Vancouver, BC, Canada, April 30 - May 3, 2018, Conference Track Proceedings*, 2018.
 - [18] Krishnamurthy Dvijotham, Sven Gowal, Robert Stanforth, Relja Arandjelovic, Brendan O’Donoghue, Jonathan Uesato, and Pushmeet Kohli. Training verified learners with learned verifiers, 2018.
 - [19] Marc Fischer, Maximilian Baader, and Martin T. Vechev. Scalable certified segmentation via randomized smoothing. *CoRR*, abs/2107.00228, 2021. URL <https://arxiv.org/abs/2107.00228>.
 - [20] Morgan Frearson and Kien Nguyen. Adversarial attack on facial recognition using visible light. *arXiv preprint arXiv:2011.12680*, 2020.
 - [21] Adam Gleave, Michael Dennis, Cody Wild, Neel Kant, Sergey Levine, and Stuart Russell. Adversarial policies: Attacking deep reinforcement learning. In *8th International Conference on Learning Representations, ICLR 2020, Addis Ababa, Ethiopia, April 26-30, 2020*. OpenReview.net, 2020. URL <https://openreview.net/forum?id=HJgEMpVFwB>.
 - [22] Zhitao Gong, Wenlu Wang, and Wei-Shinn Ku. Adversarial and clean data are not twins. *CoRR*, abs/1704.04960, 2017.
 - [23] Ian J. Goodfellow, Jonathon Shlens, and Christian Szegedy. Explaining and harnessing adversarial examples. In *3rd International Conference on Learning Representations, ICLR 2015, San Diego, CA, USA, May 7-9, 2015, Conference Track Proceedings*, 2015.
 - [24] Sven Gowal, Krishnamurthy Dvijotham, Robert Stanforth, Rudy Bunel, Chongli Qin, Jonathan Uesato, Relja Arandjelovic, Timothy Mann, and Pushmeet Kohli. On the effectiveness of interval bound propagation for training verifiably robust models, 2018.
 - [25] Kathrin Grosse, Praveen Manoharan, Nicolas Papernot, Michael Backes, and Patrick D. McDaniel. On the (statistical) detection of adversarial examples. *CoRR*, abs/1702.06280, 2017.
 - [26] Chuan Guo, Mayank Rana, Moustapha Cissé, and Laurens van der Maaten. Countering adversarial images using input transformations. In *6th International Conference on Learning Representations, ICLR 2018, Vancouver, BC, Canada, April 30 - May 3, 2018, Conference Track Proceedings*, 2018.
 - [27] Xiang He, Sibe Yang, Guanbin Li, Haofeng Li, Huiyou Chang, and Yizhou Yu. Non-local context encoder: Robust biomedical image segmentation against adversarial attacks. *CoRR*, abs/1904.12181, 2019. URL <http://arxiv.org/abs/1904.12181>.
 - [28] Po-Sen Huang, Robert Stanforth, Johannes Welbl, Chris Dyer, Dani Yogatama, Sven Gowal, Krishnamurthy Dvijotham, and Pushmeet Kohli. Achieving verified robustness to symbol substitutions via interval bound propagation. In *Proceedings of the 2019 Conference on Empirical Methods in Natural Language Processing and the 9th International Joint Conference on Natural Language Processing, EMNLP-IJCNLP 2019, Hong Kong, China, November 3-7, 2019*, pages 4081–4091, 2019. doi: 10.18653/v1/D19-1419. URL <https://doi.org/10.18653/v1/D19-1419>.
 - [29] Sandy H. Huang, Nicolas Papernot, Ian J. Goodfellow, Yan Duan, and Pieter Abbeel. Adversarial attacks on neural network policies. In *5th International Conference on Learning Representations, ICLR 2017, Toulon, France, April 24-26, 2017, Workshop Track Proceedings*. OpenReview.net, 2017. URL <https://openreview.net/forum?id=ryv1RyBK1>.

- [30] Xu Kang, Bin Song, Xiaojiang Du, and Mohsen Guizani. Adversarial attacks for image segmentation on multiple lightweight models. *IEEE Access*, 8:31359–31370, 2020. doi: 10.1109/ACCESS.2020.2973069.
- [31] Jernej Kos, Ian Fischer, and Dawn Song. Adversarial examples for generative models. In *2018 IEEE Security and Privacy Workshops, SP Workshops 2018, San Francisco, CA, USA, May 24, 2018*, pages 36–42. IEEE Computer Society, 2018. doi: 10.1109/SPW.2018.00014. URL <https://doi.org/10.1109/SPW.2018.00014>.
- [32] Alex Krizhevsky, Vinod Nair, and Geoffrey Hinton. Cifar-10 (canadian institute for advanced research). URL <http://www.cs.toronto.edu/~kriz/cifar.html>.
- [33] Aounon Kumar, Alexander Levine, Soheil Feizi, and Tom Goldstein. Certifying confidence via randomized smoothing. In Hugo Larochelle, Marc’Aurelio Ranzato, Raia Hadsell, Maria-Florina Balcan, and Hsuan-Tien Lin, editors, *Advances in Neural Information Processing Systems 33: Annual Conference on Neural Information Processing Systems 2020, NeurIPS 2020, December 6-12, 2020, virtual*, 2020. URL <https://proceedings.neurips.cc/paper/2020/hash/37aa5dfc44ddd0d19d4311e2c7a0240-Abstract.html>.
- [34] Alexey Kurakin, Ian J. Goodfellow, and Samy Bengio. Adversarial machine learning at scale. In *5th International Conference on Learning Representations, ICLR 2017, Toulon, France, April 24-26, 2017, Conference Track Proceedings*, 2017. URL <https://openreview.net/forum?id=BJm4T4Kgx>.
- [35] Cassidy Laidlaw and Soheil Feizi. Functional adversarial attacks. In Hanna M. Wallach, Hugo Larochelle, Alina Beygelzimer, Florence d’Alché-Buc, Emily B. Fox, and Roman Garnett, editors, *Advances in Neural Information Processing Systems 32: Annual Conference on Neural Information Processing Systems 2019, NeurIPS 2019, 8-14 December 2019, Vancouver, BC, Canada*, pages 10408–10418, 2019. URL <http://papers.nips.cc/paper/9228-functional-adversarial-attacks>.
- [36] Mathias Lécuyer, Vaggelis Atlidakis, Roxana Geambasu, Daniel Hsu, and Suman Jana. Certified robustness to adversarial examples with differential privacy. In *2019 IEEE Symposium on Security and Privacy, SP 2019, San Francisco, CA, USA, May 19-23, 2019*, pages 656–672, 2019.
- [37] Guang-He Lee, Yang Yuan, Shiyu Chang, and Tommi S. Jaakkola. Tight certificates of adversarial robustness for randomly smoothed classifiers. In *Advances in Neural Information Processing Systems 32: Annual Conference on Neural Information Processing Systems 2019, NeurIPS 2019, 8-14 December 2019, Vancouver, BC, Canada*, pages 4911–4922, 2019.
- [38] Alexander Levine and Soheil Feizi. Wasserstein smoothing: Certified robustness against wasserstein adversarial attacks, 2019.
- [39] Alexander Levine and Soheil Feizi. (de)randomized smoothing for certifiable defense against patch attacks. *CoRR*, abs/2002.10733, 2020. URL <https://arxiv.org/abs/2002.10733>.
- [40] Alexander Levine and Soheil Feizi. Robustness certificates for sparse adversarial attacks by randomized ablation. In *The Thirty-Fourth AAAI Conference on Artificial Intelligence, AAAI 2020, The Thirty-Second Innovative Applications of Artificial Intelligence Conference, IAAI 2020, The Tenth AAAI Symposium on Educational Advances in Artificial Intelligence, EAAI 2020, New York, NY, USA, February 7-12, 2020*, pages 4585–4593. AAAI Press, 2020. URL <https://aaai.org/ojs/index.php/AAAI/article/view/5888>.
- [41] Alexander Levine, Aounon Kumar, Thomas Goldstein, and Soheil Feizi. Tight second-order certificates for randomized smoothing, 2020.
- [42] Bai Li, Changyou Chen, Wenlin Wang, and Lawrence Carin. Certified adversarial robustness with additive noise. In *Advances in Neural Information Processing Systems 32: Annual Conference on Neural Information Processing Systems 2019, NeurIPS 2019, 8-14 December 2019, Vancouver, BC, Canada*, pages 9459–9469, 2019.
- [43] Bai Li, Changyou Chen, Wenlin Wang, and Lawrence Carin. Second-order adversarial attack and certifiable robustness, 2019. URL <https://openreview.net/forum?id=SyxaYsAqY7>.
- [44] Xin Li and Fuxin Li. Adversarial examples detection in deep networks with convolutional filter statistics. In *IEEE International Conference on Computer Vision, ICCV 2017, Venice, Italy, October 22-29, 2017*, pages 5775–5783, 2017.

- [45] Ziwei Liu, Ping Luo, Xiaogang Wang, and Xiaoou Tang. Deep learning face attributes in the wild. In *Proceedings of International Conference on Computer Vision (ICCV)*, December 2015.
- [46] Aleksander Madry, Aleksandar Makelov, Ludwig Schmidt, Dimitris Tsipras, and Adrian Vladu. Towards deep learning models resistant to adversarial attacks. In *6th International Conference on Learning Representations, ICLR 2018, Vancouver, BC, Canada, April 30 - May 3, 2018, Conference Track Proceedings*, 2018.
- [47] Matthew Mirman, Timon Gehr, and Martin Vechev. Differentiable abstract interpretation for provably robust neural networks. In Jennifer Dy and Andreas Krause, editors, *Proceedings of the 35th International Conference on Machine Learning*, volume 80 of *Proceedings of Machine Learning Research*, pages 3578–3586. PMLR, 10–15 Jul 2018. URL <http://proceedings.mlr.press/v80/mirman18b.html>.
- [48] Anay Pattanaik, Zhenyi Tang, Shuijing Liu, Gautham Bommannan, and Girish Chowdhary. Robust deep reinforcement learning with adversarial attacks. In Elisabeth André, Sven Koenig, Mehdi Dastani, and Gita Sukthankar, editors, *Proceedings of the 17th International Conference on Autonomous Agents and MultiAgent Systems, AAMAS 2018, Stockholm, Sweden, July 10-15, 2018*, pages 2040–2042. International Foundation for Autonomous Agents and Multiagent Systems Richland, SC, USA / ACM, 2018. URL <http://dl.acm.org/citation.cfm?id=3238064>.
- [49] Aditi Raghunathan, Jacob Steinhardt, and Percy Liang. Semidefinite relaxations for certifying robustness to adversarial examples. In *Proceedings of the 32nd International Conference on Neural Information Processing Systems, NIPS’18*, page 10900–10910, Red Hook, NY, USA, 2018. Curran Associates Inc.
- [50] Ankit Raj, Yoram Bresler, and Bo Li. Improving robustness of deep-learning-based image reconstruction. In *Proceedings of the 37th International Conference on Machine Learning, ICML 2020, 13-18 July 2020, Virtual Event*, volume 119 of *Proceedings of Machine Learning Research*, pages 7932–7942. PMLR, 2020. URL <http://proceedings.mlr.press/v119/raj20a.html>.
- [51] Hadi Salman, Jerry Li, Ilya P. Razenshteyn, Pengchuan Zhang, Huan Zhang, Sébastien Bubeck, and Greg Yang. Provably robust deep learning via adversarially trained smoothed classifiers. In *Advances in Neural Information Processing Systems 32: Annual Conference on Neural Information Processing Systems 2019, NeurIPS 2019, 8-14 December 2019, Vancouver, BC, Canada*, pages 11289–11300, 2019.
- [52] Vladimir Shenmaier. Complexity and approximation of the smallest k-enclosing ball problem. *European Journal of Combinatorics*, 48:81 – 87, 2015. ISSN 0195-6698. doi: <https://doi.org/10.1016/j.ejc.2015.02.011>. URL <http://www.sciencedirect.com/science/article/pii/S0195669815000335>.
- [53] Sahil Singla and Soheil Feizi. Robustness certificates against adversarial examples for relu networks. *CoRR*, abs/1902.01235, 2019.
- [54] Sahil Singla and Soheil Feizi. Second-order provable defenses against adversarial attacks, 2020.
- [55] Qing Song, Yingqi Wu, and Lu Yang. Attacks on state-of-the-art face recognition using attentional adversarial attack generative network. *CoRR*, abs/1811.12026, 2018. URL <http://arxiv.org/abs/1811.12026>.
- [56] Christian Szegedy, Wojciech Zaremba, Ilya Sutskever, Joan Bruna, Dumitru Erhan, Ian J. Goodfellow, and Rob Fergus. Intriguing properties of neural networks. In *2nd International Conference on Learning Representations, ICLR 2014, Banff, AB, Canada, April 14-16, 2014, Conference Track Proceedings*, 2014.
- [57] Jiaye Teng, Guang-He Lee, and Yang Yuan. ℓ_1 adversarial robustness certificates: a randomized smoothing approach, 2020. URL <https://openreview.net/forum?id=H1lQIgrFDS>.
- [58] Jonathan Uesato, Brendan O’Donoghue, Pushmeet Kohli, and Aäron van den Oord. Adversarial risk and the dangers of evaluating against weak attacks. In *Proceedings of the 35th International Conference on Machine Learning, ICML 2018, Stockholm, Sweden, July 10-15, 2018*, pages 5032–5041, 2018.
- [59] Fatemeh Vakhshiteh, Raghavendra Ramachandra, and Ahmad Nickabadi. Threat of adversarial attacks on face recognition: A comprehensive survey. *arXiv preprint arXiv:2007.11709*, 2020.

- [60] Adva Wolf. Making medical image reconstruction adversarially robust. 2019. URL <http://cs229.stanford.edu/proj2019spr/report/97.pdf>.
- [61] Eric Wong and J. Zico Kolter. Provable defenses against adversarial examples via the convex outer adversarial polytope. In *Proceedings of the 35th International Conference on Machine Learning, ICML 2018, Stockholmsmässan, Stockholm, Sweden, July 10-15, 2018*, pages 5283–5292, 2018.
- [62] Ping yeh Chiang, Michael J. Curry, Ahmed Abdelkader, Aounon Kumar, John Dickerson, and Tom Goldstein. Detection as regression: Certified object detection by median smoothing, 2020.
- [63] Minghao Yin, Yongbing Zhang, Xiu Li, and Shiqi Wang. When deep fool meets deep prior: Adversarial attack on super-resolution network. In *Proceedings of the 26th ACM International Conference on Multimedia, MM ’18*, page 1930–1938, New York, NY, USA, 2018. Association for Computing Machinery. ISBN 9781450356657. doi: 10.1145/3240508.3240603. URL <https://doi.org/10.1145/3240508.3240603>.
- [64] Kaipeng Zhang, Zhanpeng Zhang, Zhifeng Li, and Yu Qiao. Joint face detection and alignment using multi-task cascaded convolutional networks. *CoRR*, abs/1604.02878, 2016. URL <http://arxiv.org/abs/1604.02878>.
- [65] Richard Zhang, Phillip Isola, Alexei A. Efros, Eli Shechtman, and Oliver Wang. The unreasonable effectiveness of deep features as a perceptual metric. In *2018 IEEE Conference on Computer Vision and Pattern Recognition, CVPR 2018, Salt Lake City, UT, USA, June 18-22, 2018*, pages 586–595. IEEE Computer Society, 2018. doi: 10.1109/CVPR.2018.00068. URL http://openaccess.thecvf.com/content_cvpr_2018/html/Zhang_The_Unreasonable_Effectiveness_CVPR_2018_paper.html.

Checklist

1. For all authors...
 - (a) Do the main claims made in the abstract and introduction accurately reflect the paper’s contributions and scope? [\[Yes\]](#)
 - (b) Did you describe the limitations of your work? [\[Yes\]](#) In the conclusion (section 6), we discuss that more work is needed to generalize our method to threat models other than ℓ_2 .
 - (c) Did you discuss any potential negative societal impacts of your work? [\[N/A\]](#) Our work aims to help make machine learning models more robust and reliable for real-world applications.
 - (d) Have you read the ethics review guidelines and ensured that your paper conforms to them? [\[Yes\]](#)
2. If you are including theoretical results...
 - (a) Did you state the full set of assumptions of all theoretical results? [\[Yes\]](#)
 - (b) Did you include complete proofs of all theoretical results? [\[Yes\]](#) Complete proofs of all theorems and lemmas can be found in the appendix.
3. If you ran experiments...
 - (a) Did you include the code, data, and instructions needed to reproduce the main experimental results (either in the supplemental material or as a URL)? [\[Yes\]](#) Code is included in the supplemental.
 - (b) Did you specify all the training details (e.g., data splits, hyperparameters, how they were chosen)? [\[Yes\]](#) In the experiments section.
 - (c) Did you report error bars (e.g., with respect to the random seed after running experiments multiple times)? [\[N/A\]](#)
 - (d) Did you include the total amount of compute and the type of resources used (e.g., type of GPUs, internal cluster, or cloud provider)? [\[Yes\]](#) In the experiments section.
4. If you are using existing assets (e.g., code, data, models) or curating/releasing new assets...
 - (a) If your work uses existing assets, did you cite the creators? [\[Yes\]](#)
 - (b) Did you mention the license of the assets? [\[N/A\]](#) We are using datasets that are available in the public domain with custom license terms that allow non-commercial use, like MNIST, CIFAR-10 and CelebA.
 - (c) Did you include any new assets either in the supplemental material or as a URL? [\[Yes\]](#) Our code is included in the supplemental.
 - (d) Did you discuss whether and how consent was obtained from people whose data you’re using/curating? [\[N/A\]](#) We are using datasets that are available in the public domain with custom license terms that allow non-commercial use, like MNIST, CIFAR-10 and CelebA.
 - (e) Did you discuss whether the data you are using/curating contains personally identifiable information or offensive content? [\[N/A\]](#)
5. If you used crowdsourcing or conducted research with human subjects...
 - (a) Did you include the full text of instructions given to participants and screenshots, if applicable? [\[N/A\]](#)
 - (b) Did you describe any potential participant risks, with links to Institutional Review Board (IRB) approvals, if applicable? [\[N/A\]](#)
 - (c) Did you include the estimated hourly wage paid to participants and the total amount spent on participant compensation? [\[N/A\]](#)